Estimation of the Production Cross Section for P50

the P50 collaboration

18 September, 2013

I. INTRODUCTION

There is no available data for production cross sections of the $p(\pi^-, D^{*-})Y_c$ reactions. Only an upper limit of $\sigma \sim 7$ nb at p_π=13 GeV/c has been reported [1]. We employ some experimental results with different processes in order to estimate the cross sections of $p(\pi^-, D^{*-})Y_c$, as follows. The inclusive J/ψ production in the pion-nucleus reaction at 16 GeV/c and 22 GeV/c has been measured, which reported (1.0±0.6) nb/nucleon and (3.0±0.6) nb/nucleon, respectively [2]. These data demonstrate that the charmed particles are produced at least at a level of ∼nb. The $N(\pi^-, J/\psi)X$ reaction is a so-called OZI-suppressed process. A similar process in strange sector, $p(\pi^-, \phi)n$, has been measured, in which the cross sections reported as (1.66±0.32) μb at 4 GeV/c [3]. The ratio to the inclusive $p(\pi^-, \phi)X$, reaction cross section can be estimated roughly ∼1/10 [4]. The cross section of $N(\pi^-, J/\psi)X$ is the 4th order of magnitude reduced than that of $p(\pi^-, \phi)X$. Since the cross section of the $p(\pi^-, K^*)\Lambda$ reaction is measured as (53±2) μb [5], applying the obtained reduction factor of 10^{-4}, it is estimated that the cross section of $p(\pi^-, D^{*-})\Lambda_c$ could be a few nb.

Associated $\Lambda_c \bar{D} X$ production cross section in the gamma-induced reaction on p at 20 GeV/c has been reported as $44 \pm 7^{+11}_{-8}$ nb [6]. The experiment has reported $D^- X$ and $D^* X$ production cross sections as $29 \pm 5^{+7}_{-5}$ and $12 \pm 2^{+3}_{-2}$, respectively. From these quantities, the cross section of $\Lambda_c \bar{D}^* X$ is as large as ∼18 nb. This number seems sizable because the cross section ratio of the photon-induced reaction to the pion-induced one is expected to be roughly 1/100.

We held dissuasions with theorists several times for plausible estimations on the production cross sections.

Considering the t-channel pseudoscalar (PS) meson exchange in the $\pi N \to VB reaction$, the cross section is given by

$$\frac{d\sigma}{d(\cos\theta)} = \frac{q}{8\pi\sqrt{s}} \frac{2G^2(E_N E_B - kq\cos\theta - m_N m_\Lambda)}{4[(pk)^2 - m_\pi^2 m_N^2]^{1/2}} \frac{k^2}{2} \times F(t), \tag{1}$$

$$G(t) = \frac{2fg}{t - m_{PS}^2}, \tag{2}$$

where k, p, and q are the momenta of incident π, N, and the momentum transfer, respectively. The quantity m_{PS} is the mass of the exchange PS meson. The coupling constants at the π-PS-V and N-PS-B vertices are represented by f and g. We take the form factor $F(t)$

as $\Lambda^4/[\Lambda^4 + (t - m_{PS})^2]$, where Λ is a cut-off parameter and is 0.7 GeV. We can estimate the cross section of the $p(\pi^-, \rho)N$ reaction as 8 mb at k=0.73 GeV/c in the center of mass (CM) frame, while that of the $p(\pi^-, D^{*-})\Lambda_c$ as 0.5 μb at k=3 GeV/c (20 GeV/c in the lab frame) [7]. If we take the square of $F(t)$, the cross section of the $p(\pi^-, D^{*-})\Lambda_c$ is reduced a order of magnitude, $\sim$20 nb.

Since the c quark mass (m_c) is greater than the QCD scale (Λ_{QCD}), one may think that the perturbative approach in QCD (pQCD) is applicable. However, many difficulties are expected. At the J-PARC kinematics (especially for $\pi + p$ option), it is challenging to obtain a reliable theoretical prediction even for the inclusive production. At present, the following issues are pointed out [8] for the reliable estimation;

1. We do not know the distribution amplitude of the charmed hadrons.

2. The Soft-QCD effects (end-point, re-scattering, etc.) would be large.

This process is more difficult to handle with pQCD than the ones with the light hadrons only. We still keep discussions so that pQCD could give us some reasonable order estimation of the cross section. In particular, the pQCD might work at a larger scattering angle region, where $|t|$ is as large as s and the hard process is expected to be more dominant.

At present, we conclude that the Reggeon exchange model could give a reasonable estimation. Therefore, we revisit the Regge theory in the next section.

II. REGGEON EXCHANGE MODEL

In the Regge theory, the differential cross section of a binary (two body) reaction shows the typical s-dependence in the limit $s \to \infty$:

$$\frac{d\sigma}{dt} = \frac{g_1^2 g_2^2}{64\pi |\mathbf{p_1}|^2 s} \Gamma^2(-\alpha(t)) \left(\frac{s}{s_0}\right)^{2\alpha(t)}, \tag{3}$$

where $\alpha(t)$ is the Regge trajectory [9] and the scale parameter s_0 stands for the square of the threshold energy in the reaction. Actually, a phenomenological approximation for the form factor $\Gamma(-\alpha(t))$ is introduced. The above formula of the cross section is applicable at the diffractive region of $|t| \ll s$, where the typical angular distribution decreases rapidly as $|t|$ increases. We ignore the t dependence of the Gamma function as $\Gamma(-\alpha(t_{\rm max}))$. As a result, the t-dependence of the cross section is expressed as the exponential function. We called this approximation as "Naive Regge" for later comparison.

A. B. Kaidalov *et al.* introduced the Reggeon exchange model for high-energy hadronic binary reactions based on the quark gluon string model picture [10]. Their expression of the cross section is:

$$\sigma \sim \Gamma^2(1 - \alpha(0)) \left(\frac{s}{s_0}\right)^{2\alpha(0)-1} \frac{1}{\Lambda} e^{\Lambda t_{\rm max}}, \tag{4}$$

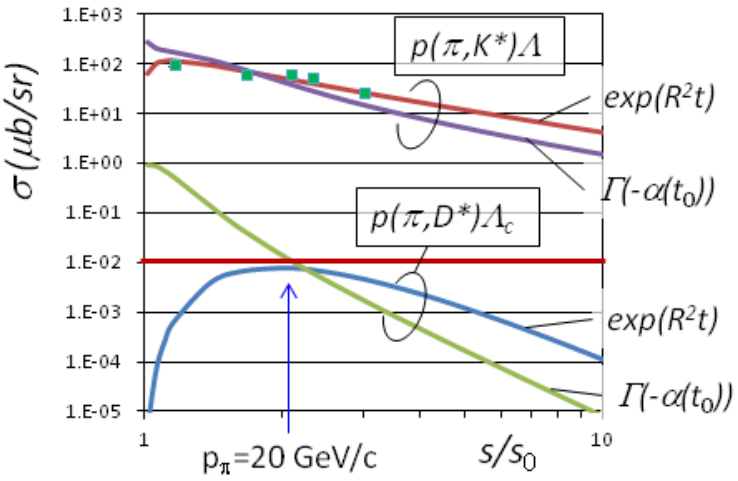

FIG. 1: Comparisons of the Naive Regge model with the Grishina's one. The cross sections are normalized so as to reproduce the experimental data of the $p(\pi^-, K^*)\Lambda$ reactions [5, 12] as plotted with closed squares.

where Λ is a parameter. Here, the scale parameter s_0 is taken much smaller than the square of the threshold energy of the reaction [10], as shown in Table III.

V. Yu. Grishina *et al*. expressed the differential cross section as

$$\frac{d\sigma}{dt} \sim \frac{g_1^2 g_2^2}{64\pi |\mathbf{p_1}|^2 s} F(t)^2 \left(\frac{s}{s_0}\right)^{2\alpha(t)}, \tag{5}$$

$$F(t) = e^{R^2 t}, \tag{6}$$

where R^2 is a parameter related to the so-called slope parameter [11]. Here, $R^2 = 2.13$ GeV^{-1} is chosen so as to reproduce the differential cross sections of pion-induced Λ hyperon production reactions in a wide range of s [11].

Comparison among the Naive Regge model, Kaidalov's model, and Grishina's model for vector reggeon exchange can be seen in Fig. 5 in Appendix A 2. The label "strange (charm)" means the $p(\pi^-, K^*)\Lambda$ ($p(\pi^-, D^{*-})\Lambda_c$) reaction, where the K^* (D^*) reggeons are considered. We obtain the ratios of the "charm" production to the "strange" one as $\sim 10^4$.

Fig. 1 compares the Naive Regge model with the Grishina's one. The cross sections are normalized so as to reproduce the experimental data of the $p(\pi^-, K^*)\Lambda$ reactions [5, 12] as plotted with closed squares. The Grishina's model with reproduces the s-dependence of the data very well. On the other hand, the Naive Regge model shows a steeper s dependence. An arrow in the figure indicates the s/s_0 values for the $p(\pi^-, D^{*-})\Lambda_c$ reaction at p=20 GeV/c, where we expect the cross section as large as 10 nb.

In the above mentioned Regge models, common (or global) coupling constants at the meson-meson-meson and baryon-baryon-meson vertices are used. Possible changes of the estimation may arise from the unknown coupling constant. A. Khodjamirian *et al*. estimate

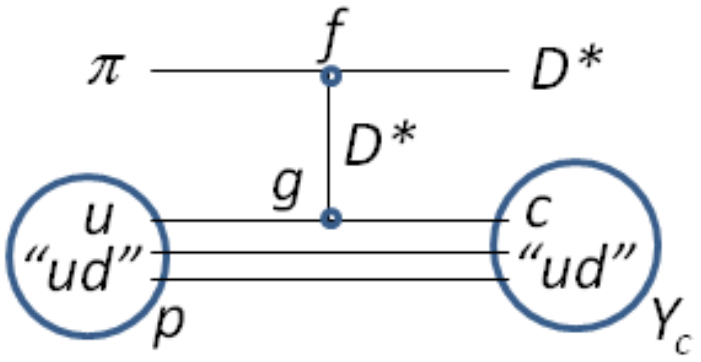

FIG. 2: Diagram of the $p(\pi^-, D^{*-})\Lambda_c$ reaction. The t-channel D^* exchange reaction is considered at a forward scattering angle.

the coupling constants as $g_{\Lambda NK^*} = -6.1^{+2.4}_{-2.0}$, $g_{\Lambda NK} = 7.3^{+2.6}_{-2.8}$, $g_{\Lambda_c ND^*} = -5.8^{+2.1}_{-2.5}$, and $g_{\Lambda_c ND} = 10.7^{+5.5}_{-4.3}$ by means of the light cone QCD sum rule (LCSR), which result in the ratios $g_{\Lambda_c ND^*}/g_{\Lambda NK^*} = 0.95^{+0.35}_{-0.28}$ and $g_{\Lambda_c ND}/g_{\Lambda NK} = 1.47^{+0.58}_{-0.44}$ [13].

The coupling constants at the vertices of three mesons are relatively well determined. M. E. Bracco *et al.* estimate the coupling constants as $g_{D^*D^*\pi} = 9$ and $g_{D^*D\pi} = 15$, by means of the LCSR [14]. Here we note that g[Bracco]/2=g[Khodjamirian] by definition. However it does not affect the present argument as far as we normalize the cross section to the experimental data in strange sector. The estimated $g_{D^*D\pi}$ is close to the measured value of $17.9 \pm 0.15 \pm -0.9$ [15]. One can obtain $g_{K^*K\pi} = 9$ from the decay width. The $g_{K^*K^*\pi}$ coupling constant can be obtained as 7 through the expression of the anomalous action in the framework of the NJL model [16]. Then, the ratios $g_{D^*D^*\pi}/g_{K^*K^*\pi} \sim 1.3$ and $g_{D^*D\pi}/g_{K^*K\pi} \sim 1.7$ are obtained.

Through the above discussion, we can estimate the ratios of the coupling constants to be $g_{\Lambda_c ND^*}/g_{\Lambda NK} \sim 0.67$ and $g_{D^*D^*\pi}/g_{K^*K^*\pi} \sim 1$ as a lower boundary. Even in this case, we can expect the cross section at a level of a few nb. The estimated cross section must be confirmed by the measurement. We consider that a few nb for the $p(\pi^-, D^{*-})\Lambda_c$ cross section is reasonable as an estimation for the present experiment.

III. EXCITATION ENERGY DEPENDENCE

We consider the t-channel D^* exchange model at a forward scattering angle in order to estimate the production rates for the excited charmed baryons, as shown in Fig. 2. Here, a u quark in the proton is converted to a c quark to form an excited charmed baryon. A ud diquark in a baryon acts as a spectator. The production rate is expressed as:

$$R \sim \gamma C |K\dot{I}|^2 p_B, \tag{7}$$

TABLE I: Production rate relative to the ground state estimated in the $p(\pi^-, D^{*-})Y_c$ reaction at $p_\pi = 20$ GeV/c.

state	$\Lambda_c^{+1/2}$	$\Sigma_c^{+1/2}$	$\Sigma_c^{+3/2}$	$\Lambda_c^{-1/2}$	$\Lambda_c^{-3/2}$	$\Sigma_c^{-1/2}$	$\Sigma_c^{-3/2}$	$\Sigma'_c{}^{-1/2}$	$\Sigma'_c{}^{-3/2}$	$\Sigma'_c{}^{-5/2}$	$\Lambda_c^{+5/2}$
(mass)	(2286)	(2455)	(2520)	(2595)	(2625)	(2750)	(2820)	(2750)	(2820)	(2820)	(2880)
γ	1/2	1/6	1/6	1/2	1/2	1/6	1/6	1/6	1/6	1/6	1/2
C	1	1/9	8/9	1/3	2/3	1/27	2/27	2/27	56/135	2/5	3/5
K	0.86	0.95	0.94	0.85	0.85	0.92	0.91	0.92	0.91	0.91	0.83
q_{eff}	1.33	1.43	1.44	1.37	1.38	1.49	1.50	1.49	1.50	1.50	1.41
R	1	0.03	0.20	1.17	2.26	0.03	0.06	0.07	0.33	0.31	1.55

where γ stands for a kind of spectroscopic factor to pick up good or bad diquark configuration in the proton. The γ equals 1/2 (1/6) for a good (bad) diquark configuration. C is a spin dependent coefficient, which is the products of the Clebush-Gordan coefficients based on the quark-diquark spin configurations in the initial and final baryon states. K is a kinematic factor expressed as:

$$K \sim k^0_{D^*} k_\pi (|\mathbf{p_B}|/2m_B - 1)/(q^2 - m^2_{D^*}), \tag{8}$$

Then, I is the overlap integral of the initial and final states.

$$I \sim \sqrt{2} \int d\mathbf{r}^3 [\varphi^*_f(\mathbf{r}) e^{\mathbf{q_{eff}} \mathbf{r}} [\varphi_i(\mathbf{r})], \tag{9}$$

$$\mathbf{q_{eff}} = \mathbf{p_p} \times \frac{m_d}{M_p} - \mathbf{p_{Y_c}} \times \frac{m_d}{M_{Y_c}}, \tag{10}$$

where $\varphi_i(\mathbf{r})$ and $\varphi_f(\mathbf{r})$ are the wave functions of the initial and final quark states, respectively. The effective momentum transfer $\mathbf{q_{eff}}$ represents a recoil effect, where m_d stands for the so-called diquark mass. Taking harmonic oscillator wave functions, I can be expressed as,

$$I \sim (q_{eff}/A)^L e^{-q^2_{eff}/2A^2}, \tag{11}$$

where A is the average of the oscillator parameters of the initial and final wave functions. A typical value of A is 0.4∼0.45 GeV. The quantity L is the orbital angular momentum of the excited baryon. This expression shows some interesting features for I. The relative strength of $I(L)$ for the excited state to $I(0)$ for the ground state is proportional to $(q_{eff}/A)^L$ if we ignore the small difference of q_{eff}/A. In the case of q_{eff} greater than A, the relative rate increases as L increases. One finds that I is maximum at $q_{eff} = \sqrt{2}A$. This can be called as the momentum matched condition. For larger q_{eff}, the absolute value of I decreases rapidly. We summarize the production rates relative to the ground state estimated in the cases of the $p(\pi^-, D^{*-})Y_c$ reaction at $p_\pi = 20$ GeV/c and $p(\pi^-, K^*)Y$ reaction at $p_\pi = 4.5$ GeV/c in Table I and Table II, respectively.

In summary of the production cross section, we remark as follows:

TABLE II: Production rate relative to the ground state estimated in the $p(\pi^-, D^{*-})Y_c$ reaction at $p_\pi = 4.5$ GeV/c. Experimental data [5] are listed for comparison.

state	$\Lambda_c^{+1/2}$	$\Sigma_c^{+1/2}$	$\Sigma_c^{+3/2}$	$\Lambda_c^{-1/2}$	$\Lambda_c^{-3/2}$
(mass)	(1116)	(1192)	(1385)	(1405)	(1520)
γ	1/2	1/6	1/6	1/2	1/2
C	1	1/9	8/9	1/3	2/3
K	1.02	1.23	1.17	0.99	0.97
q_{eff}	0.29	0.31	0.38	0.36	0.40
R	1	0.05	0.29	0.09	0.17
Exp(μb/sr)	318±12	186±28	29±6	32±7	60±13

· Estimation of the production cross section

  – The magnitude of the charm production is expected to be an order of 10^{-4} relative to the strangeness production.

  – Taking into account unknown factors of the transition form factors and the coupling constants in the $p(\pi^-, D^{*-})\Lambda_c$ reaction, a few nb for the cross section seems reasonable as an estimation for the present experiment.

· Excitation Energy Dependence

  – We demonstrated an yield estimation based on the t-channel D^* exchange scattering at a forward angle with harmonic oscillator wave functions for the initial and final quark states.

  – The present model calculation suggests that the production rate is kept even at the higher L states, depending much on spin/isospin structures of baryons.

  – We expect the signal level of ∼nb for the Λ_c states even at the higher L states, but ∼0.1 nb or less for some Σ_c states.

· We point out that a measurement of the production rates provide rich physics information;

  – The magnitudes of the coupling strength at the Y_cND^* and Y_cND vertices will be given by the production cross section.

  – The production rates of excited states with different isospin and orbital angular momentum will provide the information on the spin and radial wave functions of charmed baryons.

Note on the Charm production[22]

Abstract

We discuss charmed baryon productions induced by a high momentum pion beam. In the former part, we estimate the total production rate of the ground state charm productions as compared with the strangeness production in the Regge approach. In the latter part, we estimate ratios of various baryon productions using a quark-diquark model for baryons. This provides a characteristic feature of the production rate reflecting the spin structure of the baryons when a large momentum is transferred as compared to the inverse of baryon size.

Appendix A: Regge model

1. Amplitudes

In the Regge theory [17], the scattering amplitude is expressed by a sum over partial wave amplitudes expanded in the t-channel scattering region ($s < 0, t > 0$), which is analytically continued to the physical region of s-channel scattering ($s > 0, t < 0$). The sum over integer angular momentum l can be expressed by the Regge pole terms which are the residues of the scattering amplitude when regarded as an analytic function of the complex angular momentum l. The pole is a function of t and is expressed by $\alpha(t)$. By definition, $\alpha(t)$ reduces to an integer value at t equal to the mass square of a physical particle, $\alpha(t = nm^2) = l$, where l is regarded as the spin of the particle. Since the pole position $\alpha(t)$ moves on the complex l plane as t varies, it is often called the moving pole and its trajectory the Regge trajectory. The amplitude expressed by the Regge pole is also referred to as the Reggeon exchange amplitude.

It is shown that the amplitude obeys the asymptotic behavior in the limit $s \to \infty$ in the diffractive region of small t:

$$\langle 34|T|12\rangle \sim \text{const} \times \Gamma(-\alpha(t)) \left(\frac{s}{s_0}\right)^{\alpha(t)} \tag{A1}$$

and therefore

$$\frac{d\sigma}{dt} = \frac{\text{const}}{64\pi|_1|^2 s} \Gamma^2(-\alpha(t)) \left(\frac{s}{s_0}\right)^{2\alpha(t)} \tag{A2}$$

Indeed, we can verify that for small t the t dependence of (A2) (form factor) shows diffractive pattern. Approximating the forward peak by $\exp(\Lambda t)$ function ($\Lambda > 0, t < 0$), we can perform the t-integration to obtain the total cross section. In fact, the Γ function of (A1) is used for the pseudoscalar Reggeon exchange, while $\Gamma(1 - \alpha(t))$ is employed for vector

Reggeon exchange. As the Regge trajectory implies, the vector Reggeon dominates in the large s limit, and therefore, in the following we consider the vector Reggeon exchange.

The Regge trajectory $\alpha(t)$ is approximated by a linear function

$$\alpha(t) = \alpha_0 + \alpha' t \tag{A3}$$

in the diffractive region $t << s$.

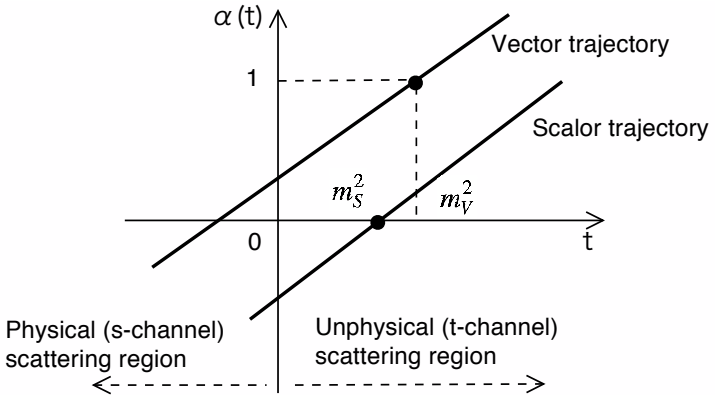

FIG. 3: Regge trajectory for scalar and vector particles. Blobs indicate the location of the corresponding lowest (band head) states.

In the t-channel scattering region ($t > 0$), consider, for example, the vector meson trajectory around the mass value, $t \sim m_V^2$,

$$\begin{aligned} \alpha(t) &= \alpha(m_V^2) + (t - m_V^2)\alpha' + \cdots \\ &= 1 + (t - m_V^2)\alpha' + \cdots \end{aligned} \tag{A4}$$

the gamma function becomes singular as

$$\Gamma(-1 - \alpha'(t - m_V^2)) \sim -\frac{1}{\alpha'(t - m_V^2)} \,, \tag{A5}$$

which is derived by the identity

$$\Gamma(x)\Gamma(1 - x) = \frac{\pi}{\sin \pi x} \tag{A6}$$

In this manner the Regge amplitude reduces to the ordinary meson exchange amplitude. This implies a method to fix the constant (const) in the Regge amplitude; determine it by identifying the Regge amplitude with that of the lowest (band head) meson exchange:

$$\begin{aligned} \langle 34|T|12\rangle &\sim -\frac{\text{const}}{\alpha'(t - m_V^2)} \\ &\to \text{lowest meson exchange amplitude} \end{aligned} \tag{A7}$$

In the present note, we do not make such determination of the absolute strengths, but rather we discuss only relative strengths of production rates.

For the Regge trajectory $\alpha(t)$, we adopt a modified function [18]

$$\alpha(t) = \alpha_0 + \gamma(\sqrt{T} - \sqrt{T-1}) \tag{A8}$$

The parameters for the pseudoscalar and vector trajectories with various flavors are summarized in Table III.

TABLE III: Various parameters for the Regge trajectory for the square root parametrization.

$\gamma = 2.68$	ud	s	c	b
$\alpha_0(P)$	-0.0118	-0.151	-1.61	-7.41
$\alpha_0(V)$	0.55	0.41	-1.02	-7.13
$\sqrt{T}(P)$	2.82	2.96	4.16	7.89
$\sqrt{T}(V)$	2.46	2.58	3.91	7.48
$s_{\pi N\to VB}$ GeV^2	1.5	1.66	4.75	27.1
$s_{\rm threshold}$(lowest) GeV^2	2.92	4.02	18.5	120

2. Comparison

The Regge's method gives the asymptotic behavior of $s \to \infty$, though its validity is not clear at low energies especially near the threshold. One ambiguity is in the choice of the scale parameter s_0. A different choice of s_0 gives a multiplicative factor

$$\left(\frac{s}{s_0'}\right)^{2\alpha(t)} = \left(\frac{s}{s_0}\right)^{2\alpha(t)} \left(\frac{s_0}{s_0'}\right)^{2\alpha(t)} \tag{A9}$$

The t dependence described by the Γ function also has limitation within ranges of small $|t|$, otherwise the Γ function may increase for large negative $\alpha(t)$ at finite scattering angles, incompatible with the diffractive pattern. To avoid such unphysical situation, Grishina introduces an exponential form $e^{-\beta t}$ for the form factor instead of the Γ function.

To see how such parameter ambiguities leads actual numerical values, we test the following three choices and evaluate the relative production rate of the strangeness and charm productions. We consider the vector Reggeon exchange where the argument of the Γ function is $1-\alpha(t)$ rather than $-\alpha(t)$.

- **Naive Regge**

  A naive formula for the vector Reggeon exchange takes the form

$$\frac{d\sigma}{dt} = \frac{\text{const}}{64\pi|p_1|^2 s}\Gamma^2(1-\alpha(t)) \left(\frac{s}{s_0}\right)^{2\alpha(t)} \tag{A10}$$

To minimize ambiguity, we adopt the Kaidalov's scale parameter s_0 [10]as summarized in Table III, $s_0 = s_{\pi N\to VB}$, depending on the production channels. They are determined by

$$s_{\pi N\to VB} = \left(s_{\pi N\to\pi N}\right)^{\frac{\alpha_\rho(0)-1}{2(\alpha_{D^*}(0)-1)}} \left(s_{VB\to VB}\right)^{\frac{\alpha_{J/\psi}(0)-1}{2(\alpha_{D^*}(0)-1)}} \tag{A11}$$

where the lower indices of α's denote the kind of the trajectory. In the topological model, the scale parameters for the flavored (off-diagonal) Reggeon exchange is expressed by an exponent average over unflavored (diagonal) Reggeon exchange, see Fig. 4.

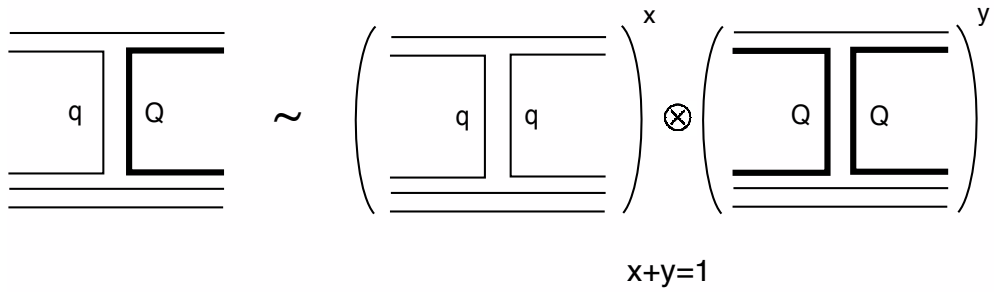

FIG. 4: Weighted average for the transverse quark masses for s_0.

- **Kaidalov's model**

  In Ref. [10] they parametrize the (t-integrated) total cross section as [10]

$$\sigma \sim \Gamma^2(1-\alpha(0)) \left(\frac{s}{s_0}\right)^{2(\alpha(0)-1)} \frac{1}{\Lambda} e^{\Lambda t_{\max}} \tag{A12}$$

  where Λ is another scale parameter. This is equivalent to the differential cross section

$$\frac{d\sigma}{dt} = \frac{\text{const}}{64\pi|p_1|^2 s} \Gamma^2(1-\alpha(t)) \left(\frac{s}{s_0}\right)^{2(\alpha(t)-1)} \tag{A13}$$

  This differs from the naive formula, due to (A9), by a multiplicative factor. Therefore, the two formulae of naive and Kaidalov give exactly the same result for all s when the absolute value is fixed at an arbitrary value of s. Nevertheless, the ratio of the charm to strangeness productions, they give different results (by a multiplicative factor) which we consider an ambiguity in the Regge's method.

- **Grishina et al**

  They parametrize the t-dependence by the exponential factor, instead of the Γ-function, but the remaining structure for the s-dependence is kept unchanged [11]

$$\frac{d\sigma}{dt} = \frac{c g_1^2 g_2^2}{64\pi|p_1|^2 s} F(t)^2 \left(\frac{s}{s_0}\right)^{2\alpha(t)} \tag{A14}$$

Here the scale parameter s_0 is taken the threshold mass of hadrons, $s_0 = m_M + m_B$. The difference in s_0 and in the form factor give somewhat different s dependence when integrated over t.

We have estimated the total cross section

$$\sigma = \int \frac{d\sigma}{dt} dt \tag{A15}$$

for the three models above. The results are compared in Fig. 5, where strange production is normalized to reproduce experimental data near the threshold. Note that the Naive and Kaidalov's models reproduce exactly the same result when they are normalized as explained before. The result of the Grishina's model is slightly shifted below for visible reason. From this, we

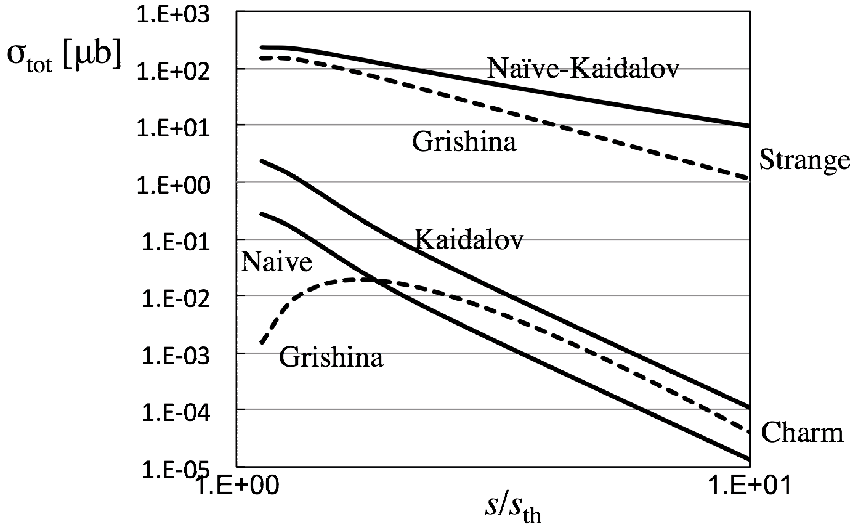

FIG. 5: Comparison among the naive Regge model, Kaidalov's model and Grishina's model for vector Reggeon exchange. The total energy square s is normalized by the threshold value $s_{th} = m_V + m_B$. For the strangeness production, $V = K^*$ and $B = \Lambda$, while for the charm production, $V = D^*$ and $B = \Lambda_c$.

Appendix B: Production rate in a quark-diquark model

1. Setups

In this section we evaluate production cross sections of various charmed baryons using a simple quark-diquark model. Our calculation here is based on several assumptions.

- We consider only the D^* exchange mechanism as shown in Fig. 6. As discussed in the previous sections of the Regge mechanism, the main contribution is expected come from the D^* (vector)-Reggeon exchange.
- We make our calculations simple by considering only the forward scattering. This makes sense when the forward (diffractive) scattering dominates as the Regge theory implies.
- Since the computation of absolute values is not easy in an effective model, we use the Regge method for it; charmed production is estimated with respect to the strange production as we have seen in the previous section. Production rates of various baryons are then used for the relative ratio, reflecting the structure of spin, isospin and orbital motion of the wave functions.
- After taking the ratio among production rates, much part of the momentum dependence in the form factor cancels. This is the dynamical part which depends on the model and on the momentum transfer entering the vertices.

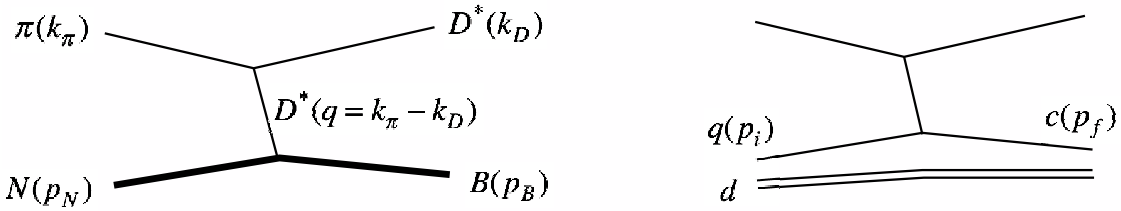

FIG. 6: The D^* exchange diagram in the t-channel for the production of D^* and charmed baryon B. Right figure shows the structure of the nucleon N and baryon B in terms of a light quark (q) and a diquark (d), and a charm quark c and the diquark.

2. Lagrangians

We use the following interaction Lagrangians,

$$\mathcal{L}_{\pi D^* D^*} = f \epsilon_{\mu\nu\alpha\beta} \partial^\mu \pi \partial^\nu D^\alpha D^\beta \tag{B1}$$

for the $\pi D^* D^*$ vertex, and

$$\mathcal{L}_{D^* qc} = g\bar{c}\gamma^\mu D_\mu q \tag{B2}$$

for the $D^* qc$ vertex. In these equations, f and g are the coupling constants, and π, D_μ, q and c represent the corresponding fields, where the star $(*)$ for D^* is suppressed for simplicity. The $\pi D^* D^*$ Lagrangian is uniquely given with the smallest number of derivatives, and is the so called anomalous (magnetic) coupling. For the $D^* qc$ coupling we adopt the vector (Dirac) type. In general the tensor coupling is also allowed when the fermion (quarks) have internal structure. However, as long as the quarks does not have structure, the tensor term is irrelevant. In our calculation we make further assumptions and approximations to make actual computation simple.

First, let us look at the $\pi D^* D^*$ coupling of (B1). When applying the Feynman rules, we need the matrix element as $\langle D^*(k_D)|\mathcal{L}_{\pi D^* D^*}|\pi(k_\pi) D^*(q)\rangle$ where q is the momentum exchanged in the t-channel and entering into the vertex. Recall that there are two ways in contracting the D^* mesons. Thus, we have the following matrix element as

$$\langle D^*(k_D)|\mathcal{L}_{\pi D^* D^*}|\pi(k_\pi) D^*(q)\rangle = 2f\epsilon_{\mu\nu\alpha\beta} k_\pi^\mu k_D^\nu e^\alpha e^\beta \tag{B3}$$

where e^α is the polarization vector of the final state D^*, while e^α is that of the exchanged D^*, and is used to form the D^* propagator. Now we assume that the charm quark, and hence D^* and B are sufficiently heavy such that their velocities in the final state are slow. In this case the time component of the momentum k_D^0 is much larger than the spatial component $k_{D^*}^i (i = 1, 2, 3)$. Thus we obtain

$$\langle \mathcal{L}_{\pi D^* D^*} \rangle \sim 2f\epsilon_{\mu 0\alpha\beta} k_\pi^\mu k_{D^*}^0 e^\alpha e^\beta \to 2f k_{D^*}^0 \vec{k}_\pi \times \vec{e} \cdot \vec{e} \tag{B4}$$

where it is understood that the first $\vec{e}$ is for the polarization vector of the final state D^* meson, while the second one is contracted for the propagator.

Next, we take a look at the $D^* qc$ Lagrangian $\mathcal{L}_{D^* qc}$. For our computation we make a reduction into a two-component form:

$$\begin{aligned} \mathcal{L}_{D^* qc} &= g\bar{c}\gamma^\mu D_\mu q \\ &= g\varphi_f^\dagger \left(1, -\frac{\vec{\sigma}\cdot\vec{p}_f}{m_c + E_c}\right) \begin{pmatrix} D^0 & -\vec{\sigma}\cdot\vec{D} \\ \vec{\sigma}\cdot\vec{D} & -D^0 \end{pmatrix} \begin{pmatrix} 1 \\ \dfrac{\vec{\sigma}\cdot\vec{p}_i}{m_q + E_q} \end{pmatrix} \varphi_i \end{aligned} \tag{B5}$$

where $\varphi_{i,f}$ are the two component spinors for the initial light quark and the final charm quark, respectively. They are confined in the baryons and are the key quantities in our calculation below. These wave functions are constructed in a non-relativistic quark-diquark model. To proceed, we pick up only terms that contain the spatial component of the D^* meson, because when this D^* meson is contracted with another from the $\pi D^* D^*$ vertex, only the spatial component survives as we have seen in Eq. (B4). Hence we find

$$\mathcal{L}_{D^* qc} \sim -g\varphi_f^\dagger \left[\left(\frac{\vec{p}_f}{m_c + E_c} + \frac{\vec{p}_i}{m_q + E_q} \right) \cdot \vec{D} + i\vec{\sigma} \times \left(\frac{\vec{p}_f}{m_c + E_c} - \frac{\vec{p}_i}{m_q + E_q} \right) \cdot \vec{D} \right] \varphi_i \tag{B6}$$

3. Amplitudes

Now combining the interaction matrix elements (B4) and (B6), we can write down the scattering amplitude for the D^* production via the D^*-exchange

$$t \sim 2fgk^0_{D^*}\vec{k}_\pi \times \vec{e}\cdot\vec{J}_{fi}\frac{1}{q^2-m^2_{D^*}} \tag{B7}$$

where $\vec{J}_{fi}$ is the baryon transition current which reflects the internal structure of the baryons. In our estimation where we employ the non-relativistic quark-diquark model, the current matrix element takes the following non-covariant form

$$\vec{J}_{fi} = \int d^3x\,\varphi^\dagger_f\left[\frac{\vec{p}_f}{m_c+E_c}+\frac{\vec{p}_i}{m_q+E_q}+i\vec{\sigma}\times\left(\frac{\vec{p}_f}{m_c+E_c}-\frac{\vec{p}_i}{m_q+E_q}\right)\right]\varphi_i\, e^{i\vec{q}_{eff}\cdot\vec{x}} \tag{B8}$$

Here we have defined the effective momentum transfer

$$\vec{q}_{eff} = \frac{m_d}{m_d+m_q}\vec{P}_N - \frac{m_d}{m_d+m_c}\vec{P}_B \tag{B9}$$

which takes into account the recoil of the center of mass motion due to the change in the masses of q and c quarks.

To further simplify the computation, we fix the quark momenta $\vec{p}_i$ and $\vec{p}_f$ at a fraction of the baryon momentum,

$$\begin{aligned}\vec{p}_i &\sim \frac{1}{3}\vec{P}_N,\\ \vec{p}_f &\sim \frac{m_c}{m_c+m_d}\vec{P}_B\end{aligned} \tag{B10}$$

Note that for the initial state the pion momentum (and hence the nucleon momentum) is sufficiently large such that the mass of the pion is neglected. Now for forward scattering where all momenta are collinear along the z-axis, only the spin current term services in the scattering amplitude (B7):

$$\begin{aligned}t_{fi} &\sim \left(\frac{P_B}{2(m_c+m_d)}-1\right)k^0_{D^*}\vec{k}_\pi\times\vec{e}\cdot\langle f|\,\vec{\sigma}\times\hat{z}\,e^{i\vec{q}_{eff}\cdot\vec{x}}\,|i\rangle\,\frac{1}{q^2-m^2_{D^*}}\\ &= \left(\frac{P_B}{2(m_c+m_d)}-1\right)k^0_{D^*}\langle f|\,\left((\vec{k}_\pi\cdot\vec{\sigma})(\vec{e}\cdot\hat{z})-(\vec{k}_\pi\cdot\hat{z})(\vec{e}\cdot\vec{\sigma})\right)e^{i\vec{q}_{eff}\cdot\vec{x}}\,|i\rangle\\ &\qquad\times\frac{1}{q^2-m^2_{D^*}}\end{aligned} \tag{B11}$$

where the collinearity of all the momenta has been used, and the constant factors which are irrelevant when taking ratios of the production rates are ignored. The polarization of D^* can be either longitudinal (z) or transverse (x,y), but the longitudinal contribution vanishes. Moreover, for the traverse polarization, the first term vanishes. Therefore, we have a rather simple form of the amplitude

$$t_{fi} \sim \left(\frac{P_B}{2(m_c+m_d)}-1\right)k^0_{D^*}k_\pi\langle f|\,\vec{e}_\perp\cdot\vec{\sigma}\,e^{i\vec{q}_{eff}\cdot\vec{x}}\,|i\rangle\,\frac{1}{q^2-m^2_{D^*}} \tag{B12}$$

where $\vec{e}_\perp$ denotes the transverse components of the D^* polarization.

4. Production rates

We have computed the transition amplitudes t_{fi} from the nucleon $N \sim i$ to various charmed baryons $B \sim f$. For charmed baryons, we consider all possible states of the ground, p-wave and d-wave excited states. The production rates are computed by

$$\mathcal{R} \sim \frac{1}{\text{Flux}} \times \sum_{fi} |t_{fi}|^2 \times \text{Phase space} \tag{B13}$$

where the phase space and flux factors are

$$\begin{aligned} \text{Phase space} &= \int (2\pi)^4 \delta^4(k_{D^*} + P_B - k_\pi - P_N) \frac{d^3k_{D^*}}{2E_{D^*}(2\pi)^3} \frac{d^3P_B}{2E_B(2\pi)^3} \\ &= \frac{q}{4\pi\sqrt{s}} \\ \text{Flux} &= 4[(p_N k_\pi)^2 - m_N^2 m_\pi^2]^{1/2} \end{aligned} \tag{B14}$$

Using the results of the amplitudes as shown in Appendix A, we find

$$\mathcal{R}(B_c(J^P)) = \frac{1}{\text{Flux}} \gamma^2 \, K^2 \, C \, |I_L|^2 \frac{q}{4\pi\sqrt{s}} \tag{B15}$$

where $I_L = I_{0,1,2}$ are computed in Appendix, and the kinematic factor is given by

$$K = k^0_{D^*} k_\pi \left(\frac{P_B}{2(m_c + m_d)} - 1 \right) \frac{1}{q^2 - m^2_{D^*}} \tag{B16}$$

The spin dependent coefficients, C are tabulated in Table IV. The overlap (spectroscopic factor) of the nucleon wave function is

$$\begin{aligned} \gamma &= \frac{1}{2} \quad \text{for } \Lambda \text{ baryons} \\ &= \frac{1}{6} \quad \text{for } \Sigma \text{ baryons} \end{aligned} \tag{B17}$$

TABLE IV: Spin dependent coefficients C for Eq. (B15).

$l=0$	$\Lambda_c(\frac{1}{2}^+)$	$\Sigma_c(\frac{1}{2}^+)$	$\Sigma_c(\frac{3}{2}^+)$					
	1	1/9	8/9					
$l=1$	$\Lambda_c(\frac{1}{2}^-)$	$\Lambda_c(\frac{3}{2}^-)$	$\Sigma_c(\frac{1}{2}^-)$	$\Sigma_c(\frac{3}{2}^-)$	$\Sigma'_c(\frac{1}{2}^-)$	$\Sigma'_c(\frac{3}{2}^-)$	$\Sigma'_c(\frac{5}{2}^-)$	
	1/3	2/3	1/27	2/27	2/27	56/135	2/5	
$l=2$	$\Lambda_c(\frac{3}{2}^+)$	$\Lambda_c(\frac{5}{2}^+-)$	$\Sigma_c(\frac{3}{2}^+)$	$\Sigma_c(\frac{5}{2}^+)$	$\Sigma'_c(\frac{1}{2}^+)$	$\Sigma'_c(\frac{3}{2}^+)$	$\Sigma'_c(\frac{5}{2}^+)$	$\Sigma'_c(\frac{5}{2}^+)$
	2/5	3/5	2/45	3/45	2/45	8/45	38/105	32/105

These coefficients C's are rather model independent, but are determined only by spin structure of the nucleon and baryons. It is interesting to see that in general the production rate of Σ baryons are small as compared to Λ baryons. This is a consequence of SU(6) symmetry which is the case also for the present quark-diquark model.

For actual production rates, we computed $\mathcal{R}(B_c(J^P))$ of (B15). Results are summarized in Table V, where numerical values are normalized by the strength $\mathcal{R}(\Lambda_c(1/2^+))$. Following observations are made:

- Λ_c excited states have similar or even larger production rates than the ground states. This is due to better overlap of the radial wave functions when the momentum transfer is large, typically of order 1 GeV and larger. For strangeness productions, the momentum transfer is much smaller, where the production of excited states are suppressed. Mathematically, this is explained by the appearance of higher power of (q_{eff}/A) as in (B13) and (B16).

- Σ_c baryons are in general suppressed as compared to Λ_c baryons because of smaller spin-flavor overlap. For the vector D^* exchange, the transverse spin transfer is needed. A similar feature holds for the pseudoscalar D exchange, where longitudinal spin is transferred.

TABLE V: Production rates $\mathcal{R}(B_c(J^P))$ normalized by $\mathcal{R}(\Lambda_c(1/2^+))$ at the pion momentum $k_\pi(lab) = 20$ GeV.

$l=0$	$\Lambda_c(\frac{1}{2}^+)$	$\Sigma_c(\frac{1}{2}^+)$	$\Sigma_c(\frac{3}{2}^+)$					
	1.00	0.03	0.20					
$l=1$	$\Lambda_c(\frac{1}{2}^-)$	$\Lambda_c(\frac{3}{2}^-)$	$\Sigma_c(\frac{1}{2}^-)$	$\Sigma_c(\frac{3}{2}^-)$	$\Sigma'_c(\frac{1}{2}^-)$	$\Sigma'_c(\frac{3}{2}^-)$	$\Sigma'_c(\frac{5}{2}^-)$	
	1.17	2.26	0.03	0.06	0.07	0.33	0.31	
$l=2$	$\Lambda_c(\frac{3}{2}^+)$	$\Lambda_c(\frac{5}{2}^+-)$	$\Sigma_c(\frac{3}{2}^+)$	$\Sigma_c(\frac{5}{2}^+)$	$\Sigma'_c(\frac{1}{2}^+)$	$\Sigma'_c(\frac{3}{2}^+)$	$\Sigma'_c(\frac{5}{2}^+)$	$\Sigma'_c(\frac{5}{2}^+)$
	0.85	1.41	0.03	0.04	0.02	0.08	0.17	0.15

Acknowledgements:

This work is partly supported by the Grant-in-Aid for Scientific Research on Priority Areas titled "Elucidation of New Hadrons with a Variety of Flavors" (E01: 21105006).

Appendix A: Cross sections

We consider a two-body process $12 \to 34$. S-matrix is related to the T-matrix by

$$S = 1 - iT \tag{A1}$$

For matrix elements, this means that

$$\langle 34|S|12\rangle = \langle 34|12\rangle - i(2\pi)^4\delta^4(p_1 + p_2 - p_3 - p_4)\langle 34|T|12\rangle \tag{A2}$$

Using this T-matrix the cross section is given by

$$d\sigma_{12\to 34} = \frac{1}{4|p_1|\sqrt{s}}\frac{d^3p_3}{2E_3(2\pi)^3}\frac{d^3p_4}{2E_4(2\pi)^3}(2\pi)^4\delta^4(p_1 + p_2 - p_3 - p_4)|\langle 34|T|12\rangle|^2 \tag{A3}$$

$E_3 = \sqrt{p_3^2 + m_3^2}$, and so on. After perfuming the integral on the right hand side, and using the relation

$$t = (p_3 - p_1)^2, \quad dt = 2|p_1||p_3|d(\cos\theta) \tag{A4}$$

we find

$$\frac{d\sigma}{dt} = \frac{1}{4|p_1|^2 s}\frac{1}{16\pi}|\langle 34|T|12\rangle|^2, \tag{A5}$$

Here the factor $4|p_1|^2 s$ is the flux of 12 and is expressed also as $4|p_1|^2 s = s(s - 4m^2)$ when $m_3 = m_4 = m$.

Appendix B: Computation of matrix elements

We calculate the matrix elements $\langle f|\,\vec{e}_\perp \cdot \vec{\sigma}\, e^{i\vec{q}_{eff}\cdot\vec{x}}\,|i\rangle$ for baryons B with various spin and parity J^P. For forward scattering, due to helicity conservation, it is sufficient consider essentially only one helicity flip transition for a given J_B (remember that we have only transverse polarization components),

$$J_z(N) \to (J_z(B), J_z(D^*)) = 1/2 \to (-1/2, 1) \tag{B1}$$

for $J_B = 1/2$ and $3/2$, and

$$J_z(N) \to (J_z(B), J_z(D^*)) = -1/2 \to (-3/2, 1) \tag{B2}$$

for $J_B = 3/2$. Other amplitudes are related to these elements by time reversal.

The total cross section is then proportional to the sum of squared amplitudes over possible spin states (with notation $t_{fi} = \langle J_z(B), J_z(D^*)|t|J_z(N)\rangle$):
For $J_B = 1/2$

$$\begin{aligned}\sigma &\sim |\langle -1/2, +1|t|+1/2\rangle|^2 + |\langle +1/2, -1|t|-1/2\rangle|^2 \\ &= 2|\langle -1/2, +1|t|+1/2\rangle|^2\end{aligned} \tag{B3}$$

and for $J_B = 3/2$ and $5/2$

$$\sigma \sim 2\left(|\langle -1/2, +1|t| + 1/2\rangle|^2 + |\langle +3/2, -1|t| + 1/2\rangle|^2\right) \tag{B4}$$

1. $N(1/2^+) \to$ ground state charmed baryons

First we consider the transition to $\Lambda_c(1/2^+)$

$$\langle \psi_{000}\chi^{\rho}_{-1/2} D^*(+1)|\vec{e}_\perp \cdot \vec{\sigma}\, e^{i\vec{q}_{eff}\cdot\vec{x}}\, |\psi_{000}\chi^{\rho}_{+1/2}\rangle \tag{B5}$$

Note that since the diquark behaves as a spectator during the reaction, the good diquark component for the nucleon is taken. The spectroscopic (overlap) factor of the good diquark component in the nucleon is tabulated in below where isospin factor is included also. Choosing the D^* polarization $\vec{e}_\perp \to \vec{e}^{\,(+)}$, we have

$$\langle \psi_{000}\chi^{\rho}_{-1/2}|\sqrt{2}\sigma_-\, e^{i\vec{q}_{eff}\cdot\vec{x}}\, |\psi_{000}\chi^{\rho}_{+1/2}\rangle = \langle \chi^{\rho}_{-1/2}|\sigma_-|\chi^{\rho}_{+1/2}\rangle\, \langle \psi_{000}|\sqrt{2}\, e^{i\vec{q}_{eff}\cdot\vec{x}}\, |\psi_{000}\rangle \tag{B6}$$

where the spin and orbital part is separated and σ_- is the Pauli lowering matrix is given as

$$\sigma_- = \begin{pmatrix} 0 & 0 \\ 1 & 0 \end{pmatrix} \tag{B7}$$

The spin matrix element in this case is easily computed as

$$\begin{aligned}
\langle \chi^{\rho}_{-1/2}|\sigma_-|\chi^{\rho}_{+1/2}\rangle &= 1, \\
\langle \chi^{\lambda}_{-1/2}|\sigma_-|\chi^{\lambda}+1/2\rangle &= -\frac{1}{3} \\
\langle \chi^{S}_{-1/2}|\sigma_-|\chi^{\lambda}+1/2\rangle &= \frac{\sqrt{2}}{3} \\
\langle \chi^{S}_{-3/2}|\sigma_-|\chi^{\lambda}-1/2\rangle &= -\sqrt{\frac{2}{3}}
\end{aligned} \tag{B8}$$

where we have tabulated all relevant matrix elements in the following calculations. Therefore, the remaining is the elementary integral over the radial distance r with Gaussian functions, and we find

$$\Lambda_c(1/2^+): \quad \langle \psi_{000}\chi^{\rho}_{-1/2}|\sqrt{2}\sigma_-\, e^{i\vec{q}_{eff}\cdot\vec{x}}\, |\psi_{000}\chi^{\rho}_{+1/2}\rangle = I_0 \tag{B9}$$

where the radial integral I_0 is given by

$$\begin{aligned}
I_0 &= \langle \psi_{000}|\sqrt{2}\, e^{i\vec{q}_{eff}\cdot\vec{x}}\, |\psi_{000}\rangle = \sqrt{2}\left(\frac{\alpha'\alpha}{A^2}\right)^{3/2} e^{-q^2_{eff}/(4A^2)} \\
A^2 &= \frac{\alpha^2 + \alpha'^2}{2}
\end{aligned} \tag{B10}$$

where in ψ and ψ', the oscillator parameters are α and α', respectively.

Similarly, we calculate the transitions to the ground state Σ_c's, with the chi^λ part for the nucleon wave function. Only the difference is the spin matrix element which are computed by making Clebsh-Gordan decompositions. Results are

$$\begin{aligned}
\Sigma_c(1/2^+): \quad & \langle\psi_{000}\chi^\lambda_{-1/2}|\sqrt{2}\sigma_- \, e^{i\vec{q}_{eff}\cdot\vec{x}}\,|\psi_{000}\chi^\lambda_{+1/2}\rangle \;=\; -\frac{1}{3}I_0 \\
\Sigma_c(3/2^+): \quad & \langle\psi_{000}\chi^S_{-1/2}|\sqrt{2}\sigma_- \, e^{i\vec{q}_{eff}\cdot\vec{x}}\,|\psi_{000}\chi^\lambda_{+1/2}\rangle \;=\; \frac{\sqrt{2}}{3}I_0 \\
& \langle\psi_{000}\chi^S_{-3/2}|\sqrt{2}\sigma_- \, e^{i\vec{q}_{eff}\cdot\vec{x}}\,|\psi_{000}\chi^\lambda_{-1/2}\rangle \;=\; -\sqrt{\frac{2}{3}}I_0
\end{aligned} \tag{B11}$$

where two independent matrix elements for $\Sigma_c(3/2^+)$ are shown.

2. $N(1/2^+) \to p$-wave charmed baryons

Let us first consider the transition to $\Lambda_c(1/2^-)$. The relevant matrix element is given as

$$\langle[\psi_{01},\chi^\rho]^{1/2}_{-1/2}|\sqrt{2}\sigma_- \, e^{i\vec{q}_{eff}\cdot\vec{x}}\,|\psi_{000}\chi^\rho_{+1/2}\rangle = \sqrt{\frac{1}{3}}\langle\chi^\rho_{-1/2}|\sigma_-|\chi^\rho_{+1/2}\rangle\,\langle\psi_{010}|\sqrt{2}\,e^{i\vec{q}_{eff}\cdot\vec{x}}\,|\psi_{000}\rangle \tag{B12}$$

where the factor $\sqrt{1/3}$ is the Clebsh-Gordan coefficients in the state $[\psi_{01},\chi^\rho]^{1/2}_{-1/2}$. The radial part is computed as

$$\langle\psi_{010}|\sqrt{2}\,e^{i\vec{q}_{eff}\cdot\vec{x}}\,|\psi_{000}\rangle = \frac{(\alpha'\alpha)^{3/2}\alpha' q_{eff}}{A^5}\,\cos\theta_{q_{eff}} e^{-q^2_{eff}/(4A^2)} \equiv I_1 \tag{B13}$$

and so

$$\Lambda_c(1/2^-): \quad \langle[\psi_{01},\chi^\rho]^{1/2}_{-1/2}|\sqrt{2}\sigma_- \, e^{i\vec{q}_{eff}\cdot\vec{x}}\,|\psi_{000}\chi^\rho_{+1/2}\rangle = \sqrt{\frac{1}{3}}\,I_1 \tag{B14}$$

Other matrix elements can be computed similarly:

$$\begin{aligned}
\Lambda_c(3/2^-): \quad & \langle[\psi_{01},\chi^\rho]^{3/2}_{-1/2}|\sqrt{2}\sigma_- \, e^{i\vec{q}_{eff}\cdot\vec{x}}\,|\psi_{000}\chi^\rho_{+1/2}\rangle = \sqrt{\frac{2}{3}}I_1 \\
& \langle[\psi_{01},\chi^\rho]^{3/2}_{-3/2}|\sqrt{2}\sigma_- \, e^{i\vec{q}_{eff}\cdot\vec{x}}\,|\psi_{000}\chi^\rho_{-1/2}\rangle = 0 \\
\Sigma_c(1/2^-): \quad & \langle[\psi_{01},\chi^\lambda]^{3/2}_{-1/2}|\sqrt{2}\sigma_- \, e^{i\vec{q}_{eff}\cdot\vec{x}}\,|\psi_{000}\chi^\lambda_{+1/2}\rangle = \frac{1}{3\sqrt{3}}I_1 \\
\Sigma_c(3/2^-): \quad & \langle[\psi_{01},\chi^\lambda]^{3/2}_{-1/2}|\sqrt{2}\sigma_- \, e^{i\vec{q}_{eff}\cdot\vec{x}}\,|\psi_{000}\chi^\lambda_{+1/2}\rangle = -\frac{1}{3}\sqrt{\frac{2}{3}}I_1 \\
& \langle[\psi_{01},\chi^\lambda]^{3/2}_{-3/2}|\sqrt{2}\sigma_- \, e^{i\vec{q}_{eff}\cdot\vec{x}}\,|\psi_{000}\chi^\lambda_{-1/2}\rangle = 0 \\
\Sigma'_c(1/2^-): \quad & \langle[\psi_{01},\chi^S]^{1/2}_{-1/2}|\sqrt{2}\sigma_- \, e^{i\vec{q}_{eff}\cdot\vec{x}}\,|\psi_{000}\chi^\lambda_{+1/2}\rangle = -\frac{1}{3}\sqrt{\frac{2}{3}}I_1
\end{aligned}$$

$$
\begin{aligned}
\Sigma_c'(3/2^-): \quad & \langle[\psi_{01},\chi^S]^{3/2}_{-1/2}|\sqrt{2}\sigma_-\, e^{i\vec{q}_{eff}\cdot\vec{x}}\,|\psi_{000}\chi^\lambda_{+1/2}\rangle = \frac{1}{3}\sqrt{\frac{2}{15}}I_1 \\
& \langle[\psi_{01},\chi^S]^{3/2}_{-3/2}|\sqrt{2}\sigma_-\, e^{i\vec{q}_{eff}\cdot\vec{x}}\,|\psi_{000}\chi^\lambda_{-1/2}\rangle = \sqrt{\frac{2}{5}}I_1 \\
\Sigma_c'(5/2^-): \quad & \langle[\psi_{01},\chi^S]^{5/2}_{-1/2}|\sqrt{2}\sigma_-\, e^{i\vec{q}_{eff}\cdot\vec{x}}\,|\psi_{000}\chi^\lambda_{+1/2}\rangle = -\sqrt{\frac{2}{15}}I_1 \\
& \langle[\psi_{01},\chi^S]^{5/2}_{-3/2}|\sqrt{2}\sigma_-\, e^{i\vec{q}_{eff}\cdot\vec{x}}\,|\psi_{000}\chi^\lambda_{-1/2}\rangle = -\sqrt{\frac{4}{15}}I_1
\end{aligned}
\tag{B15}
$$

3. $N(1/2^+) \to d$-wave charmed baryons

Computations go in completely similar manner as before, except for the radial matrix element

$$
\langle\psi_{020}|\sqrt{2}\, e^{i\vec{q}_{eff}\cdot\vec{x}}\,|\psi_{000}\rangle = \frac{1}{2}\sqrt{\frac{2}{3}}\frac{(\alpha\alpha')^{3/2}}{A^3}\left(\frac{\alpha' q}{A^2}\right)^2 e^{-q^2_{eff}/(4A^2)} \equiv I_2 \tag{B16}
$$

The results are

$$
\begin{aligned}
\Lambda_c(3/2^+): \quad & \langle[\psi_{02},\chi^\rho]^{3/2}_{-1/2}|\sqrt{2}\sigma_-\, e^{i\vec{q}_{eff}\cdot\vec{x}}\,|\psi_{000}\chi^\rho_{+1/2}\rangle = -\sqrt{\frac{2}{5}}I_2 \\
& \langle[\psi_{02},\chi^\rho]^{3/2}_{-3/2}|\sqrt{2}\sigma_-\, e^{i\vec{q}_{eff}\cdot\vec{x}}\,|\psi_{000}\chi^\rho_{-1/2}\rangle = 0 \\
\Lambda_c(5/2^+): \quad & \langle[\psi_{02},\chi^\rho]^{5/2}_{-1/2}|\sqrt{2}\sigma_-\, e^{i\vec{q}_{eff}\cdot\vec{x}}\,|\psi_{000}\chi^\rho_{+1/2}\rangle = \sqrt{\frac{3}{5}}I_2 \\
& \langle[\psi_{02},\chi^\rho]^{5/2}_{-3/2}|\sqrt{2}\sigma_-\, e^{i\vec{q}_{eff}\cdot\vec{x}}\,|\psi_{000}\chi^\rho_{-1/2}\rangle = 0 \\
\Sigma_c(3/2^+): \quad & \langle[\psi_{02},\chi^\lambda]^{3/2}_{-1/2}|\sqrt{2}\sigma_-\, e^{i\vec{q}_{eff}\cdot\vec{x}}\,|\psi_{000}\chi^\lambda_{+1/2}\rangle = \sqrt{\frac{3}{5}}I_2 \\
& \langle[\psi_{02},\chi^\lambda]^{3/2}_{-3/2}|\sqrt{2}\sigma_-\, e^{i\vec{q}_{eff}\cdot\vec{x}}\,|\psi_{000}\chi^\lambda_{-1/2}\rangle = 0 \\
\Sigma_c(5/2^+): \quad & \langle[\psi_{02},\chi^\lambda]^{5/2}_{-1/2}|\sqrt{2}\sigma_-\, e^{i\vec{q}_{eff}\cdot\vec{x}}\,|\psi_{000}\chi^\lambda_{+1/2}\rangle = \sqrt{\frac{3}{5}}I_2 \\
& \langle[\psi_{02},\chi^\lambda]^{5/2}_{-3/2}|\sqrt{2}\sigma_-\, e^{i\vec{q}_{eff}\cdot\vec{x}}\,|\psi_{000}\chi^\lambda_{-1/2}\rangle = 0 \\
\Sigma_c'(1/2^+): \quad & \langle[\psi_{02},\chi^S]^{1/2}_{-1/2}|\sqrt{2}\sigma_-\, e^{i\vec{q}_{eff}\cdot\vec{x}}\,|\psi_{000}\chi^\lambda_{+1/2}\rangle = \sqrt{\frac{3}{5}}I_2 \\
\Sigma_c'(3/2^+): \quad & \langle[\psi_{02},\chi^S]^{3/2}_{-1/2}|\sqrt{2}\sigma_-\, e^{i\vec{q}_{eff}\cdot\vec{x}}\,|\psi_{000}\chi^\lambda_{+1/2}\rangle = \sqrt{\frac{3}{5}}I_2 \\
& \langle[\psi_{02},\chi^S]^{3/2}_{-3/2}|\sqrt{2}\sigma_-\, e^{i\vec{q}_{eff}\cdot\vec{x}}\,|\psi_{000}\chi^\lambda_{-1/2}\rangle = 0 \\
\Sigma_c'(5/2^+): \quad & \langle[\psi_{02},\chi^S]^{5/2}_{-1/2}|\sqrt{2}\sigma_-\, e^{i\vec{q}_{eff}\cdot\vec{x}}\,|\psi_{000}\chi^\lambda_{+1/2}\rangle = \sqrt{\frac{3}{5}}I_2 \\
& \langle[\psi_{02},\chi^S]^{5/2}_{-3/2}|\sqrt{2}\sigma_-\, e^{i\vec{q}_{eff}\cdot\vec{x}}\,|\psi_{000}\chi^\lambda_{-1/2}\rangle = 0
\end{aligned}
$$

$$\Sigma_c'(7/2^+): \quad \langle[\psi_{02},\chi^S]^{7/2}_{-1/2}|\sqrt{2}\sigma_- \, e^{i\vec{q}_{eff}\cdot\vec{x}}\,|\psi_{000}\chi^\lambda_{+1/2}\rangle = \sqrt{\frac{3}{5}}I_2$$
$$\langle[\psi_{02},\chi^S]^{7/2}_{-3/2}|\sqrt{2}\sigma_- \, e^{i\vec{q}_{eff}\cdot\vec{x}}\,|\psi_{000}\chi^\lambda_{-1/2}\rangle = 0 \tag{B17}$$

Appendix C: Baryon wave functions

We summarize the baryon wave functions which appear in the reactions [21]. They are constructed by a quark and a diquark, and are expresses as products of isospin, spin and orbital wave functions. Here we show explicitly spin and orbital parts. For orbital wave functions, we employ harmonic oscillator functions as given in appendix D.

For spin wave functions, we follow the notations and employ the three functions

$$\begin{aligned}\chi^\rho_m &= [d^0,\chi]^{1/2}_m\,,\\ \chi^\lambda_m &= [d^1,\chi]^{1/2}_m\,,\\ \chi^S_m &= [d^1,\chi]^{3/2}_m\end{aligned} \tag{C1}$$

where d^J_m is the diquark spin function of (Jm) and χ the two component spinor. In this note, we consider the following nine charmed baryons. For the ground states we have three states

$$\begin{aligned}\Lambda_c(1/2^+,m) &= \psi_{000}(\vec{x})\chi^\rho_m\\ \Sigma_c(1/2^+,m) &= \psi_{000}(\vec{x})\chi^\lambda_m\\ \Sigma_c(3/2^+,m) &= \psi_{000}(\vec{x})\chi^S_m\end{aligned} \tag{C2}$$

For the first excited states of negative parity there are six states ($\psi_{nlm}\to\psi_{nl}=\psi_{01}$)

$$\begin{aligned}\Lambda_c(1/2^-,m) &= [\psi_{01}(\vec{x}),\chi^\rho]^{1/2}_m\\ \Lambda_c(3/2^-,m) &= [\psi_{01}(\vec{x}),\chi^\rho]^{3/2}_m\\ \Sigma_c(1/2^-,m) &= [\psi_{01}(\vec{x}),\chi^\lambda]^{1/2}_m\\ \Sigma_c(3/2^-,m) &= [\psi_{01}(\vec{x}),\chi^\lambda]^{3/2}_m\\ \Sigma_c'(1/2^-,m) &= [\psi_{01}(\vec{x}),\chi^S]^{1/2}_m\\ \Sigma_c'(3/2^-,m) &= [\psi_{01}(\vec{x}),\chi^S]^{3/2}_m\\ \Sigma_c'(5/2^-,m) &= [\psi_{01}(\vec{x}),\chi^S]^{5/2}_m\end{aligned} \tag{C3}$$

Similarly, we obtain the wave functions for the $l=2$ excited baryons.

The nucleon wave function is written in the SU(3) wave function which contains both χ^ρ and χ^λ spin parts with an isospin wave function multiplied (this part is not written here explicitly). Denoting that part by ϕ^ρ and ϕ^λ, the nucleon wave function is written as

$$N = \psi_{000}\frac{1}{\sqrt{2}}\left(\chi^\rho\phi^\rho+\chi^\lambda\phi^\lambda\right) \tag{C4}$$

Appendix D: Harmonic oscillator wave functions

We summarize some of the harmonic oscillator wave functions for low lying states. Including the angular and radial parts, it is given as

$$\psi_{nlm}(\vec{x}) = Y_{lm}(\hat{x})R_{nl}(r) \tag{D1}$$

where $R_{nl}(r)$ are

$$\begin{aligned}
R_{00}(r) &= \frac{\alpha^{3/2}}{\pi^{1/4}} 2e^{-(\alpha^2/2)r^2} \\
R_{01}(r) &= \frac{\alpha^{3/2}}{\pi^{1/4}} \left(\frac{8}{3}\right)^{1/2} \alpha r e^{-(\alpha^2/2)r^2} \\
R_{10}(r) &= \frac{\alpha^{3/2}}{\pi^{1/4}} (2\cdot 3)^{1/2} \left(1 - \frac{2}{3}(\alpha r)^2\right) e^{-(\alpha^2/2)r^2} \\
R_{02}(r) &= \frac{\alpha^{3/2}}{\pi^{1/4}} \left(\frac{16}{5\cdot 3}\right)^{1/2} (\alpha r)^2 e^{-(\alpha^2/2)r^2}
\end{aligned} \tag{D2}$$

The oscillator parameter α misrelated to the frequency ω by

$$\alpha = \sqrt{m\omega} = (km)^{1/4} \tag{D3}$$

where k is the spring constant.

[1] J. H. Christensen *et al.*, Phys. Rev. Lett. **55**, 154(1985).
[2] J. LeBritton *et al.*, Phys. Lett. **81**B, 401(1979).
[3] D. S. Ayrez *et al.*, Phys. Rev. Lett **32** 1463 (1973).
[4] D. J. Gidal *et al.*, Phys. Rev. D **17** 1256 (1978).
[5] D. J. Crennell *et al.*, Phys. Rev. D **6** 1220 (1972).
[6] K. Abe *et al.*, Phys. Rev. D **33** 1 (1986).
[7] A. Hosaka, private communication (2013).
[8] H. Kawamura, private communication (2013).
[9] M. M. Brisudova, L. Burakovsky, and T. Goldman, Phys. Rev. D **61**, 054013(2000).
[10] A. B. Kaidalov, Z. Phys. C **12**, 63 (1982); .
[11] V. Yu. Grishina *et al.*, Euro. J. Phys. A **25**, 141 (2005).
[12] O. I. Dahl *et al.*, Phys. Rev. **163** 1377(1967).
[13] A. Khodjamirian *et al.*, Euro. J. Phys. A **48**, 31 (2012).
[14] M. E. Bracco *et al.*, Prog. Part. Nucl. Phys. **67**, 1019 (2012).
[15] V. M. Belyaev *et al.*, Phys. Rev. D**51** 6177(1995).
[16] T. Fujiwara *et al.*, Prog. Theor. Phys. **73**, 962 (1985).
[17] A. Donnachie, H.G. Dosch, P.V. Landshoff and O. Nachtmann, "Pomeron Physics and QCD", Cambridge University Press, 2002.
[18] M. M. Brisudova, L. Burakovsky and J. T. Goldman, Phys. Rev. D **61**, 054013 (2000) [hep-ph/9906293].
[19] A. B. Kaidalov and P. E. Volkovitsky, Z. Phys. C **63**, 517 (1994).
[20] V. Y. .Grishina, L. A. Kondratyuk, W. Cassing, M. Mirazita and P. Rossi, Eur. Phys. J. A **25**, 141 (2005) [nucl-th/0506053].
[21] A. Hosaka and H. Toki, "Quarks, baryons and chiral symmetry", World Scientific, 2001.
Eur. Phys. J. A **25**, 141 (2005) [nucl-th/0506053].
[22] Atsushi Hosaka, *Research Center for Nuclear Physics (RCNP), Osaka University, Ibaraki, 567-0047, Japan*